Transfer of $CuInS_2$ layer by lift-off process and its solar cell applications

Yasuhiro Abe[1], Shintaro Osada[2], Shohei Fukamizu[2], Yusuke Oda[2], Takashi Minemoto[1, 2],
Koji Nakanishi[3], Toshiaki Ohta[3], Hideyuki Takakura[2]

1) Ritsumeikan Global Innovation Research Organization, Ritsumeikan University,
2) College of Science and Engineering, Ritsumeikan University,
3) The SR Center, Ritsumeikan University

According to the PV 2030+ of new energy and industrial technology development organization (NEDO), Japan, a conversion efficiency of 25% is required for $CuInSe_2$-based chalcopyrite semiconductor thin film solar cells in 2017 [1]. Since a conversion efficiency of over 30% was achieved in a tandem structure solar cell using III-V based semiconductors [2], a tandem structure solar cell is one of promising candidates even in $CuInSe_2$-based chalcopyrite semiconductor thin film solar cells [3-6]. Unfortunately, conversion efficiencies of the tandem solar cells are still lower than those of the single junction solar cells [3-6]. In particular, several groups indicated that the fabrication of the high efficiency top solar cells with the wide band gap absorber layers such as $CuGaSe_2$ and $Cu(In,Ga)S_2$ on the transparent back electrodes was difficult due to the low temperature growth [3,6]. We think that mechanical stack using a lift-off process is attractive as the preparation method of the top solar cell, because the high quality absorber layer, which is grown on a conventional Mo/soda-lime glass (SLG) substrate at the appropriate growth temperature, can be prepared. Establishment of the lift-off process for the $CuInS_2$-based thin films which suit the absorber layer of the top solar cell [7] is therefore required.

In this study, we investigated the peeling of a $CuInS_2$ layer grown on a Mo/SLG substrate. In addition, we fabricated the superstrate-type $CuInS_2$ solar cell by transcribing a substrate-type $CuInS_2$ solar cell. In this paper, we report on the peeling of the $CuInS_2$ layer and characteristics of the superstrate-type $CuInS_2$ solar cell.

A schematic illustration of a transfer sample is shown in Fig. 1(a). The transfer sample of a $CuInS_2$ layer was fabricated as follows. An 800-nm-thick Mo layer was deposited on an SLG substrate by the radio frequency (RF) magnetron sputtering method without intentional substrate heating. A 3.5-µm-thick $CuInS_2$ layer was grown on the Mo/SLG substrate at 550˚C by the vacuum coevaporation method [8]. An alternative SLG substrate was bonded onto the $CuInS_2$ surface with cyanoacrylate glue. The alternative SLG substrate was vertically separated from the primary SLG substrate by tensile strain [9].

The schematic illustrations of the superstrate-type and substrate-type $CuInS_2$ solar cells are shown in Figs. 1(b) and 1(c), respectively. The fabrication procedure of the superstrate-type $CuInS_2$ solar cell is as follows [10]. After the

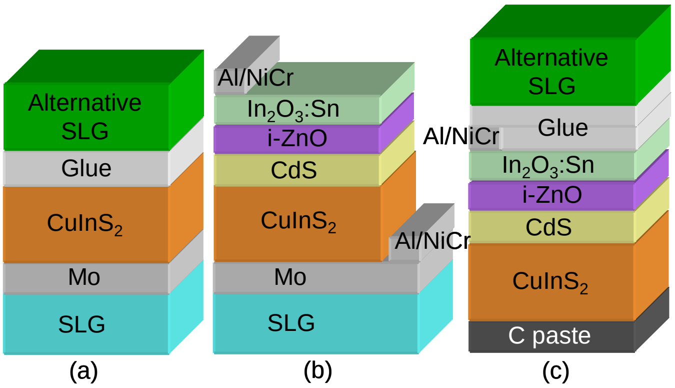

Fig. 1. Schematic illustrations of fabricated samples. (a) Lift-off sample, (b) substrate-type $CuInS_2$ solar cell, and (c) superstrate-type $CuInS_2$ solar cell.

2-μm-thick $CuInS_2$/Mo/SLG structure was fabricated through the above procedure, the samples were dipped into a KCN solution to remove Cu sulfide compounds. A 100-nm-thick CdS layer was deposited by the chemical bath deposition method. 100-nm-thick i-ZnO/200-nm-thick In_2O_3:Sn layers were deposited by the RF magnetron sputtering method. An Al/NiCr grid was formed by heat resistance deposition method using a shadow mask. An alternative SLG substrate was bonded onto this substrate-type solar cell surface with ultraviolet glue with light transparency. The lift-off process was performed. After a graphite paste was applied as a back electrode, the sample was annealed at 120˚C for 1 h in the atmosphere to dry the graphite back electrode.

Grazing incident x-ray diffraction (GIXRD) and x-ray absorption fine structure (XAFS) spectroscopy measurements were performed to identify the part separated by the lift-off process. XAFS spectroscopy measurements were performed at BL-10 of the SR center at Ritsumeikan University, Japan [11]. S K-edge x-ray absorption near edge structure (XANES) spectra were measured at room temperature under vacuum conditions. In this experiment, a double crystal Ge(111) monochromator was utilized. We used the total electron yield (TEY) method for the surface-sensitive analysis. Current density-voltage (*J*-*V*) measurements were performed under standard air mass 1.5 global conditions (100 mW/cm^2) at 25˚C to investigate performance of the fabricated solar cells. For comparison, the substrate-type $CuInS_2$ solar cells were also measured before the lift-off process.

Figure 2 shows GIXRD patterns of the $CuInS_2$ rear and Mo sides. Peaks of $CuInS_2$ only are detected for the $CuInS_2$ rear side. On the other hand, peaks of Mo only are detected for the Mo side. We therefore have to interpret that this peeling occurred at the Mo/$CuInS_2$ interface from this CIXRD result.

Figure 3 shows S K-edge XANES spectra of the $CuInS_2$ rear and Mo sides. The result of a high purity single crystalline MoS_2 reagent is also shown for comparison. The XANES spectrum of the $CuInS_2$ rear side is remarkably different from that of the Mo side. On the other hand, the XANES spectrum of the Mo side is very similar to that of the MoS_2 reagent. We found that MoS_2 formed at the surface of the Mo side. Moreover, we found that the XANES spectrum of the Mo side hardly included the component of $CuInS_2$. On the other hand, if an ultrathin MoS_2 layer exists on the surface of the $CuInS_2$ rear side, the MoS_2 component can not be recognized because of relatively high intensity of the $CuInS_2$ spectrum compared to the MoS_2 component. This result therefore indicates that peeling of the $CuInS_2$ layer occurred at the $CuInS_2$/MoS_2 interface or through breaking of the interfacial MoS_2 layer at the $CuInS_2$/Mo interface. Since breaking of the $CuInS_2$ layer does not occur in the transfer

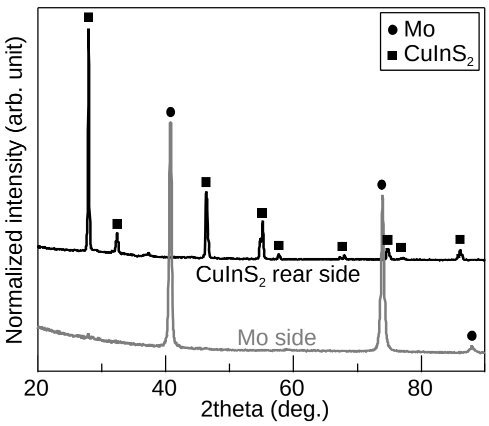

Fig. 2. GIXRD patterns of $CuInS_2$ rear and Mo sides.

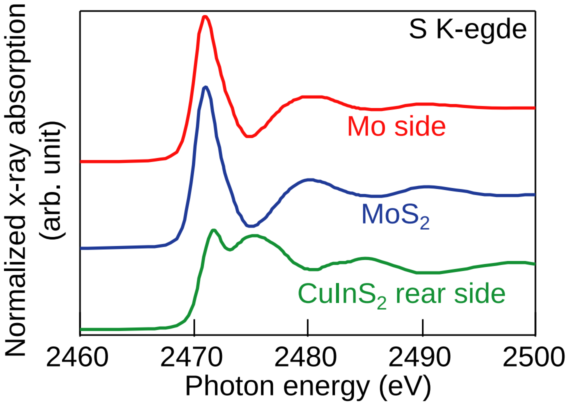

Fig. 3. S K-edge XANES spectra of Mo and $CuInS_2$ rear sides. MoS_2 reagent result is also shown for comparison.

of the $CuInS_2$ layer, it is easy to control the eventual thickness of the transferred $CuInS_2$ layer.

Figure 4 shows the *J*-*V* characteristic of the superstrate-type $CuInS_2$ solar cell fabricated by transcribing the substrate-type $CuInS_2$ solar cell. The *J*-*V* characteristic of the substrate-type $CuInS_2$ solar cell before the lift-off process is also shown in Fig. 4 for comparison. A conversion efficiency of the substrate-type solar cell is very close to that of the superstrate-type solar cell. We therefore established the lift-off process without remarkable degradation of a conversion efficiency for a $CuInS_2$ thin film solar cell.

We investigated how the $CuInS_2$ layer was peeled by the lift-off process in the transfer of the $CuInS_2$ layer grown on the Mo/SLG substrate. Our result indicates that the peeling of the $CuInS_2$ layer occurred at the $CuInS_2/MoS_2$ interface or through breaking of the MoS_2 layer. Moreover, we investigated the solar cell performance of the superstrate-type $CuInS_2$ solar cell fabricated by transcribing the substrate-type $CuInS_2$ solar cell. We found that the conversion efficiency of the substrate-type solar cell is very close to that of the superstrate-type solar cell. We therefore established the lift-off process without remarkable degradation of a conversion efficiency for the $CuInS_2$ thin film solar cell.

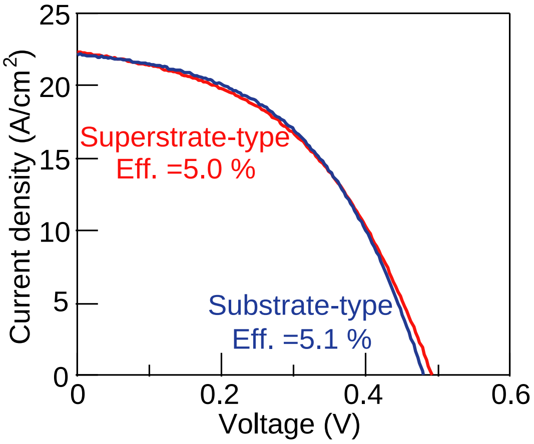

Fig. 4. *J*-*V* characteristics of superstrate-type and substrate-type $CuInS_2$ solar cells.

Acknowledgements

This work was conducted in the research group of “Thin Film Full Spectrum Solar Cells with Low Concentration Ratios” in Research and Development on Innovative Solar Cells of NEDO, Japan. XAFS measurements of this work were supported by Nanotechnology Network Project of the Ministry of Education, Culture, Sports, Science and Technology (MEXT), Japan.

References

[1] *PV2030+*, New Energy and Industrial Technology Development Organization, 2009 http://www.nedo.go.jp/library/pv2030/pv2030+.pdf.

[2] T. Takamoto, E. Ikeda, H. Kurita, and M. Ohmori, *Appl. Phys. Lett.* **70**, 301 (1997).

[3] D. L.Young, J. Abushama, R. Noufi, L. Xiaonan, J. Keane, T. A. Gessert, J. S. Ward, M. Contreras, M. Symko-Davies, and T. J. Coutts, *Conference record of the Twenty-Ninth IEEE Photovoltaic Specialists Conference*, New Orleans, pp. 608, (2002).

[4] S. Nishiwaki, S. Siebentritt, P. Walk, and M. Ch. Lux-Steiner, *Prog. Photovolt. Res. Appl.* **11**, 243 (2003).

[5] T. Nakada, S. Kijima, Y. Kuromiya, R. Arai, Y. Ishii, N. Kawamura, H. Ishizaki, and N. Yamada, *Conference Record of the 2006 IEEE Forth World Conference on Photovoltaic Energy Conversion*, Hawaii, pp. 400 (2006).

[6] R. Kaigawa, K. Funahashi, R. Fujie, T. Wada, S. Merdes, R. Caballero, and R. Klenk, *Sol. Energy Mater. Sol. Cells* **94**, 1880 (2010).

[7] Y. Oda, T. Kondo, S. Fukamizu, T. Minemoto, and H. Takakura, *RENEWABLE ENERGY 2010 Proceedings*, Yokohama, pp. P-Pv-68 (2010).
[8] S. Fukamizu, T. Kondo, Y. Oda, T. Minemoto, and H. Takakura, *Jpn. J. Appl. Phys.* (in press).
[9] T. Anegawa, Y. Oda, T. Minemoto, and H. Takakura, *J. Cryst. Growth* **311**, 742 (2009).
[10] S. Osada, Y. Abe, T. Anegawa, T. Minemoto, and H. Takakura, *Sol. Energy Mater. Sol. Cells* **95**, 223 (2011).
[11] K. Nakanishi and T. Ohta, *J. Phys.: Condens. Matter* **21**, 104214 (2009).